

# Reservoir-Engineered Exceptional Points for Quantum Energy Storage

Borhan Ahmadi<sup>1,\*</sup>, André H. A. Malavazi<sup>1,†</sup>, Paweł Mazurek<sup>2</sup>, Paweł Horodecki<sup>1</sup> and Shabir Barzanjeh<sup>3,‡</sup>

<sup>1</sup>*International Centre for Theory of Quantum Technologies,*

*University of Gdańsk, Jana Bażyńskiego 8, 80-309 Gdańsk, Poland*

<sup>2</sup>*Institute of Informatics, Faculty of Mathematics, Physics and Informatics,*

*University of Gdańsk, Wita Stwosza 63, 80-308 Gdańsk, Poland*

<sup>3</sup>*Department of Physics and Astronomy, University of Calgary, Calgary, AB T2N 1N4 Canada*

(Dated: November 26, 2025)

Exceptional points are spectral singularities where both eigenvalues and eigenvectors collapse onto a single mode, causing the system's behaviour to shift abruptly and making it highly responsive to even small perturbations. Although widely studied in optical and quantum systems, using them for energy storage in quantum systems has been difficult because existing approaches rely on gain, precise balanced loss, or explicitly non-Hermitian Hamiltonians. Here we introduce a quantum energy-storage mechanism that realizes exceptional-point physics in a fully passive, physically consistent open quantum system. Instead of amplification, we use trace-preserving reservoir engineering to create an effective complex interaction between a charging mode and a storage mode through a dissipative mediator, generating an exceptional point directly in the drift matrix of the Heisenberg–Langevin equations while preserving complete positivity. The resulting dynamics exhibit two regimes: a stable phase where the stored energy saturates, and a broken phase where energy grows exponentially under a bounded coherent drive. This rapid charging arises from dissipative interference that greatly boosts energy flow between the modes without gain media or nonlinear amplification. The mechanism is compatible with optomechanical devices, superconducting circuits, and magnonic systems, offering a practical route to fast, robust, and scalable quantum energy-storage technologies and new directions in quantum thermodynamics.

*Introduction*— Singularities represent critical points in parameter space where the behavior of a physical system changes in a fundamentally non-analytic way relative to its surroundings [1]. Among these, exceptional points (EPs) are spectral singularities of non-Hermitian systems, where two or more eigenvalues—and their associated eigenvectors—coalesce [1, 2]. These degeneracies have since been recognized as physically rich features that profoundly alter the dynamics of open systems [3–5]. Near EPs, infinitesimal parameter variations can induce macroscopic changes in eigenvalue spectra and energy flow, enabling abrupt transitions, enhanced sensitivity, and nontrivial topological behavior [2, 4, 6–10].

Beyond their mathematical elegance, EPs have become experimentally accessible platforms for exploring the interplay between coherence, dissipation, and topology across optics, photonics, and condensed-matter systems. In photonic platforms, carefully engineered gain–loss profiles realize parity–time (PT) symmetry, which undergoes spontaneous symmetry breaking at an EP [3, 4, 11]. These transitions have enabled effects such as unidirectional invisibility [12], mode-selective lasing [13, 14], coherent perfect absorption [15, 16], and topologically protected mode conversion [17]. In cavity and circuit QED, EPs reshape energy-transfer pathways, supporting unconventional amplification and robust control of system dynamics [18, 19].

In this work, we demonstrate a pathway to EP physics in quantum devices that avoids the need for explicit gain–loss mechanisms. By employing trace-preserving reservoir engineering, we induce spectral coalescence characteristic of EPs and leverage it to mediate energy transfer and storage between two coupled quantum modes. This engineered dissipation enables efficient and coherent energy dynamics, laying the groundwork for practical EP-assisted quantum batteries.

Quantum batteries (QBs) [20–27]—devices that store and release energy through coherent or correlated quantum processes—are rapidly emerging as a core target for quantum technologies [28–48]. Their deployment hinges on fast, efficient charging while preserving coherence. Most EP-assisted schemes to date rely on explicitly non-Hermitian Hamiltonians or PT-symmetric dimers [34, 35], where exponential energy growth is achieved via amplification processes. These designs typically demand strong nonlinearities or intense pumping—conditions that are often incompatible with fragile quantum systems. In practice, operating near an EP also increases noise sensitivity, demands a tight gain–loss balance, and risks saturation, pump depletion, and dynamical instabilities; thermal loading and reservoir coupling reduce fidelity, and non-orthogonal modes complicate readout and control [2, 4, 7].

We propose an EP-enabled storage paradigm that preserves complete positivity, trace, and thermodynamic consistency. Exponential charging arises in a passive, fully open quantum system by inducing EPs through reservoir engineering [49–52], without invoking explicit gain or non-Hermitian Hamiltonians. In this system,

\* [borhan.ahmadi@ug.edu.pl](mailto:borhan.ahmadi@ug.edu.pl)

† [andrehmalavazi@gmail.com](mailto:andrehmalavazi@gmail.com)

‡ [shabir.barzanjeh@ucalgary.ca](mailto:shabir.barzanjeh@ucalgary.ca)

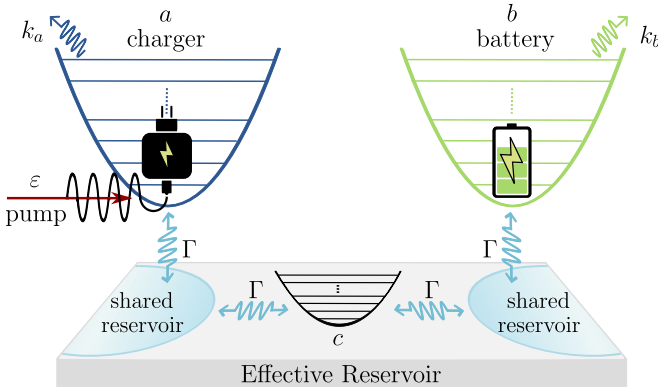


FIG. 1: Schematic of the dissipative quantum battery. A harmonic oscillator with resonance frequency  $\omega_a$  and damping rate  $\kappa_a$  serves as the charger and is driven by a classical field of frequency  $\omega_L$  and amplitude  $\mathcal{E}$ , which supplies energy to the system. The charger interacts dissipatively with a second mode, the battery, characterized by resonance frequency  $\omega_b$  and damping rate  $\kappa_b$ , where the injected energy is ultimately stored. Their interaction is mediated by an auxiliary dissipative mode  $c$ , defined by resonance frequency  $\omega_c$  and damping rate  $\kappa_c$ . When the charger and the battery both couple to mode  $c$  via two nonlocal reservoirs with coupling rate  $\Gamma$ , a purely dissipative interaction between them is induced. By adiabatically eliminating mode  $c$ , this configuration effectively engineers a reservoir that mediates the dissipative coupling between the two modes.

a carefully engineered dissipative environment facilitates efficient energy transfer between the charger and quantum battery modes. By incorporating an engineered reservoir, such as an auxiliary lossy waveguide, we induce a controlled dissipative interaction that mediates coupling between the two modes. This mediated process creates an effective complex coupling, causing dynamical eigenmodes in the Heisenberg–Langevin description to coalesce and thereby realize an EP within a physically consistent open-system framework.

The system exhibits two distinct dynamical phases. In the stable phase, the energy stored in the quantum battery saturates at a finite value. In the broken phase, the stored energy increases exponentially over time, even though the system is driven only by a bounded coherent pump. This rapid energy growth arises from dissipative interference near the engineered exceptional point, where the engineered reservoir creates correlated pathways that enhance energy transfer between the charger and the battery. This mechanism enables fast and efficient energy storage in the quantum battery without requiring external amplification or non-Hermitian gain. Our proposal can be implemented in opto-electromechanical [53, 54] superconducting [55, 56] or magnonic [57, 58] circuits, offering a practical and scalable route to EP-enhanced quantum energy storage that avoids the instability, noise amplification, and delicate calibration associated with

gain–loss EP implementations.

*The Model—* Figure 4 shows the schematic of the system. A harmonic oscillator with resonance frequency  $\omega_a$  and local damping rate  $\kappa_a$  plays the role of the charger. It interacts dissipatively with a second mode acting as the battery, characterized by a resonance frequency  $\omega_b$  and a damping rate  $\kappa_b$ . The charger is driven by a classical field of frequency  $\omega_L$  and amplitude  $\mathcal{E}$ , which provides the energy ultimately stored in the battery. We assume that the charger and battery do not exchange energy through any direct coherent coupling. In the frame rotating at the pump frequency, the non-interacting Hamiltonian of the system is given by  $\hat{H}_0 = \sum_{j=a,b} \delta_j \hat{j}^\dagger \hat{j} + \mathcal{E} (\hat{a}^\dagger + \hat{a})$ , where  $\delta_j = \omega_j - \omega_L$  with  $\hbar = 1$ .

The interaction between the charger and the battery is mediated by a dissipative auxiliary mode  $c$ , characterized by a resonance frequency  $\omega_c$  and damping rate  $\kappa_c$ , with Hamiltonian  $\hat{H}_c = \delta_c \hat{c}^\dagger \hat{c}$ . This strongly overdamped mode acts as a controllable, engineered reservoir that induces a purely dissipative coupling between the two subsystems. As explained in the Supplementary Materials, this arises when both the charger and the battery are coupled to  $c$  through two nonlocal reservoirs with coupling rate  $\Gamma$ , producing an effective dissipative interaction between them [59].

Assuming a Markovian reservoir, the system dynamics follow the master equation  $\dot{\hat{\rho}} = -i[\hat{H}_0, \hat{\rho}] + \sum_{j=a,b,c} \kappa_j \mathcal{D}_j[\hat{\rho}] + \Gamma (\mathcal{D}_{za}[\hat{\rho}] + \mathcal{D}_{zb}[\hat{\rho}])$ , where  $\mathcal{D}_o[\hat{\rho}] = \hat{\rho} \hat{o} \hat{o}^\dagger - \frac{1}{2} \{\hat{o}^\dagger \hat{o}, \hat{\rho}\}$  is the dissipative superoperator. The operators  $\hat{z}_j = p_j \hat{j} + p_c^{(j)} \hat{c}$  ( $j = a, b$ ) describe the coupling to the shared reservoir, with  $p_j$  and  $p_c^{(j)}$  being the respective coupling strengths [59]. The first term in the master equation describes the coherent dynamics of the charger and battery, while the second term accounts for the local damping of each mode into its individual bath at rates  $\kappa_{a/b/c}$ . The last two terms represent the dissipation of the mode pairs  $(a, c)$  and  $(b, c)$  into their respective shared reservoirs, which in turn generates the effective dissipative coupling between these mode pairs. Such engineered couplings can be implemented by realizing the shared reservoir as a damped cavity, a waveguide, or a transmission line [54, 57, 58]. We note that, for simplicity, we restrict our analysis to a Markovian reservoir; however, dissipative interactions can also be created in non-Markovian regimes, as studied in Ref. [60].

In the experimentally relevant regime where the mode  $c$  relaxes much faster than the modes  $a$  and  $b$  (i.e.,  $\kappa_c + \Gamma_c \gg \{\kappa_{a,b} + \Gamma_{a,b}, |\delta_{a,b}|\}$ ), we adiabatically eliminate  $c$ , which leads to a fully dissipative coupling between the charger and the battery with an effective rate  $\Gamma_{\text{eff}} = \Gamma^2 / (\kappa_c + \Gamma_c)$ , as described in the Supplementary Materials. In this reduced description, and assuming  $\delta_a = -\delta_b = \delta$ , the charger-battery equations of motion can be written as

$$\Gamma_{\text{eff}}^{-1} \frac{d}{dt} \begin{pmatrix} a \\ b \end{pmatrix} = -i \mathbb{H}_r \begin{pmatrix} a \\ b \end{pmatrix} + \begin{pmatrix} \mathcal{E}_r \\ 0 \end{pmatrix}, \quad (1)$$

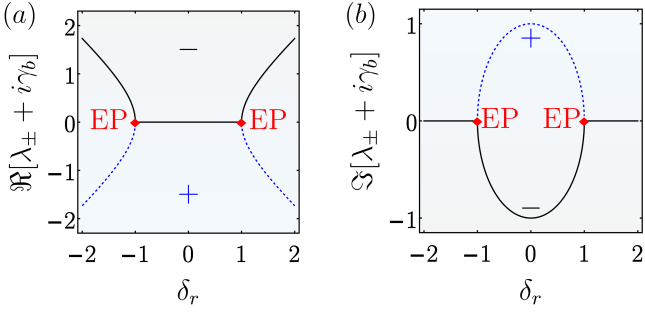


FIG. 2: (a) Real and (b) imaginary parts of the eigenvalues  $\lambda_+$  (dashed blue) and  $\lambda_-$  (solid black) of  $\mathbb{H}_r$  displaced by  $i\gamma_b$  as a function of  $\delta_r$  for symmetric damping rates  $\alpha = 0$ . The red diamond at  $\delta_r = \pm 1$  indicates the exceptional point (EP) where the eigenvalues coalesce.

where  $o := \text{Tr} \{ \hat{\rho} \hat{\rho} \}$ ,  $\mathcal{E}_r = \mathcal{E}/\Gamma_{\text{eff}}$  and

$$\mathbb{H}_r = \begin{pmatrix} \delta_r - i\gamma_a & i \\ i & -\delta_r - i\gamma_b \end{pmatrix}, \quad (2)$$

with  $\gamma_j = \Gamma_{\text{eff}}^{-1}(\kappa_j + \Gamma_j - \mu_{cj}^2 \Gamma_{\text{eff}})$ ,  $\mu_{cj} = p_c^{(j)} p_j^*$  ( $j = a, b$ ),  $\Gamma_j = \Gamma|p_j|^2$ , and  $\delta_r = \Gamma_{\text{eff}}^{-1}\delta$ . Rescaling time as  $t \rightarrow \Gamma_{\text{eff}}t$  allows us to work with the normalized matrix  $\mathbb{H}_r$  in what follows. Moreover, provided all  $p_j$  are nonzero, we may rescale them such that  $|\mu_{cj}| = 1$ , since any remaining factor can be absorbed into  $\Gamma$ . The total damping rate of the charger and battery,  $\gamma_j \geq 0$ , contains contributions from their local damping to individual reservoirs,  $\kappa_j$ , and from their coupling to the shared reservoirs,  $\Gamma_j$ . The final term, proportional to  $\Gamma_{\text{eff}}$  and appearing with a negative sign, reflects the footprint of the eliminated mode  $c$ . From a system-reservoir perspective, this negative term originates from interference between multiple dissipation pathways. The auxiliary mode  $c$ , which is itself coupled to engineered reservoirs, introduces an additional frequency-dependent decay channel for the slow modes. Eliminating  $c$  generates retarded self-interactions and cross-dissipative processes whose contributions to the drift matrix enter with a phase opposite to that of the bare local losses. In the reduced two-mode description, this interference appears as negative contributions to the effective damping rates, similar to optical dynamical backaction in cavity optomechanics [61] and to reservoir-engineered amplifiers [5, 59] where dissipative and coherent interactions combine to produce effective negative damping of a collective mode.

Now we can calculate the energy stored in the battery by solving Eq. (1), leading to (see Supplementary Materials)

$$E_B(t) = \mathcal{E}_r^2 \left| \frac{\lambda_+ e^{-i\lambda_- t} - \lambda_- e^{-i\lambda_+ t} - \Delta_{\lambda}}{\Pi_{\lambda} \Delta_{\lambda}} \right|^2, \quad (3)$$

where  $\Pi_{\lambda} = \lambda_+ \lambda_-$  and  $\Delta_{\lambda} \equiv \lambda_+ - \lambda_- = 2\Omega$ . The corresponding eigenvalues of the matrix  $\mathbb{H}_r$  are  $\lambda_{\pm} = -i(\alpha +$

$\gamma_b) \pm \Omega$ , with eigenvectors  $\mathbf{v}_{\pm} = [-\alpha - i(\delta_r \pm \Omega), 1]^T$ . Here  $\Omega = i\sqrt{1 + (\alpha + i\delta_r)^2}$  and  $\alpha = (\gamma_a - \gamma_b)/2$ .

Equation (3) shows that the stored energy in the battery depends directly on the eigenvalues of the drift matrix  $\mathbb{H}_r$ . This provides a natural way to understand how energy is shared between the charger and the battery near, or exactly at, exceptional points, where the system undergoes a dynamical phase transition in a  $\mathcal{PT}$ -inspired sense adapted to our open Heisenberg–Langevin setting. Figure 2 displays the real (a) and imaginary (b) parts of  $i\gamma_b + (\lambda_{\pm})$  as functions of  $\delta_r$  for  $\alpha = 0$ , with EPs marked by red diamonds indicating the coalescence points. In what follows, we examine how the battery energy scales in three regimes: at the EP, where  $\lambda_- = \lambda_+$ ; in the unbroken regime, defined by  $\Re[-i\lambda_+] < 0$ ; and in the broken regime, defined by  $\Re[-i\lambda_+] > 0$ .

In the EP regime,  $\Omega = 0$ , the eigenvalues and eigenvectors of  $\mathbb{H}_r$  coalesce, yielding  $\lambda_+ = \lambda_- = -i\gamma$  and  $\mathbf{v}_+ = \mathbf{v}_- = [-i\delta_r, 1]^T$ , with  $\gamma := \gamma_a = \gamma_b$  at  $\delta_r = \pm 1$ , as illustrated in Fig. 2(a). At this singular operating point, the system dynamics collapse onto a single defective mode, and the battery evolution acquires the characteristic polynomial-exponential structure of EP dynamics. The stored energy takes the explicit form

$$E_B^{\text{EP}}(t) = \mathcal{E}_r^2 \left| \frac{ie^{-i\sqrt{\Pi_0}t}}{\sqrt{\Pi_0}} \left( t - \frac{i}{\sqrt{\Pi_0}} \right) - \frac{1}{\Pi_0} \right|^2, \quad (4)$$

where  $\Pi_0 = \Pi_{\lambda}(\alpha = 0, \Omega = 0)$ . The energy grows algebraically at short times, reflecting the coalescence of eigenmodes, before settling into its long-time value  $\lim_{t \rightarrow \infty} E_B^{\text{EP}}(t) = (\mathcal{E}_r/\Pi_0)^2$ . Even at this singularity, the system remains dynamically stable and the battery converges to a finite steady state.

Away from the exceptional point, stability persists throughout the unbroken-symmetry regime, where  $\Re[-i\lambda_+] < 0$ . Here the real part of the collective eigenfrequency remains negative, ensuring that the exponential contributions to the dynamics decay in time. This behavior is most transparent in the special case  $\alpha = 0$ , for which

$$E_B^{\text{un}}(t) = \frac{\mathcal{E}_r^2}{\mathcal{K}^2} \left( 1 - \frac{e^{-\gamma t}}{\Omega} [\gamma \sin(\Omega t) + \Omega \cos(\Omega t)] \right)^2, \quad (5)$$

with  $\mathcal{K} = \delta_r^2 + \gamma^2 - 1$ . In this regime, the battery energy is strictly bounded and relaxes monotonically toward  $\lim_{t \rightarrow \infty} E_B^{\text{un}}(t) = (\mathcal{E}_r/\mathcal{K})^2$ . Both the EP and unbroken regimes therefore support stable operation. This is fully consistent with the Routh–Hurwitz criterion [62], which yields the same stability requirement  $\Re[-i\lambda_+] < 0$ .

Instability emerges only once the system crosses into the broken regime, where the condition  $\Re[-i\lambda_+] < 0$  is violated and the dominant eigenvalue instead satisfies  $\Re[-i\lambda_+] > 0$ . In this parameter region, the collective mode acquires a positive real frequency component, leading to an exponential amplification of the system's dynamics. Consequently, the battery energy no

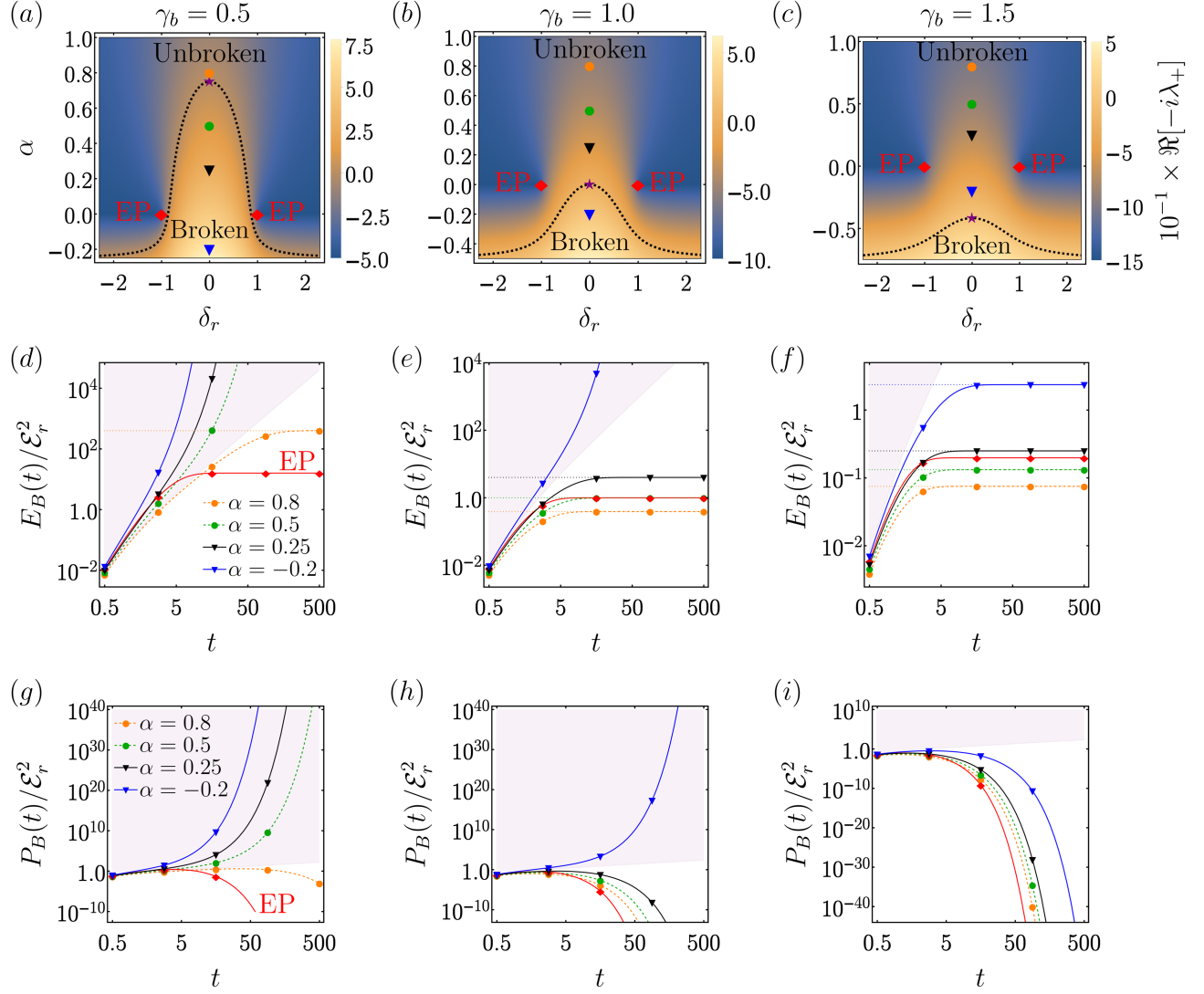


FIG. 3: (a)-(c) Phase diagrams illustrating  $\Re[-i\lambda_+]$  in terms of  $\delta_r$  and  $\alpha \geq -\gamma_b/2$  for fixed (a)  $\gamma_b = 0.5$ , (b)  $\gamma_b = 1.0$  and (c)  $\gamma_b = 1.5$ . The black dashed line indicates the transition boundary between the unbroken ( $\mathcal{PT}$ -symmetric) phase and the broken ( $\mathcal{PT}$ -broken) phase, the purple star highlights this point for  $\delta_r = 0$ . The red diamonds mark the Exceptional Points (EPs), where the eigenvalues coalesce. The blue, black, green, and orange markers represent specific parameter points for which the dynamics are plotted in panels below. (d)-(f) present the energy dynamics assuming  $\delta_r = 0$  and distinct values of  $\alpha$ . The purple filling indicates the region with exponential energy growth. (g)-(i) Normalized rate of energy change in the battery  $P_B(t)$ , showing exponential growth in the broken regime and a bounded rate that decays to zero in the unbroken regime.

longer saturates but grows without bound, driven by the unstable eigenmode. Physically, this corresponds to the engineered reservoir funneling excitations back into the charger–battery subsystem through dissipative interference. The auxiliary reservoir reinforces, rather than attenuates, the energy-exchange pathway, overwhelming the intrinsic losses and giving rise to a runaway amplification process that characterizes the broken-symmetry phase.

In this regime, the structure of the solution changes qualitatively. The oscillatory response of the unbroken

phase is replaced by hyperbolic growth, reflecting the real-valued nature of the unstable eigenfrequency. For the special case  $\alpha = 0$ , the energy stored in the battery takes the explicit form

$$E_B^{\text{br}}(t) = \frac{E_r^2}{\mathcal{K}^2} \left( 1 - \frac{e^{-\gamma t}}{|\Omega|} [\gamma \sinh(|\Omega|t) + |\Omega| \cosh(|\Omega|t)] \right)^2, \quad (6)$$

which makes the exponential divergence of the broken-symmetry dynamics explicit through the hyperbolic functions  $\sinh(|\Omega|t)$  and  $\cosh(|\Omega|t)$ . In the asymptotic limit of  $t \gg |\Omega|^{-1}$  hyperbolic terms are dominated by the growth

ing exponential,  $\sinh(x) \approx \cosh(x) \approx e^x/2$ . Thus, the energy stored in the battery simplifies to

$$E_B^{\text{br}}(t) \approx \frac{\mathcal{E}_r^2}{\mathcal{K}^2} \left( \frac{\gamma + |\Omega|}{2|\Omega|} \right)^2 e^{2(|\Omega| - \gamma)t}. \quad (7)$$

Note that in the broken regime we have  $\Re[-i\lambda_+] > 0$ , which implies  $\Re[-i\Omega] > \alpha + \gamma_b$ . For  $\alpha = 0$  this condition reduces to  $|\Omega| > \gamma$  in which  $E_B^{\text{br}}(t)$  is an exponentially growing function.

To illustrate the dynamical behavior of the system and its correspondence to the different symmetry phases discussed above, Fig. 3(a)–(c) shows the phase diagram of  $\Re[-i\lambda_+]$  versus  $\delta_r$  and  $\alpha$  for  $\alpha \geq -\gamma_b/2$  and for three fixed values of the battery damping rate: (a)  $\gamma_b = 0.5$ , (b)  $\gamma_b = 1$ , and (c)  $\gamma_b = 2.5$ . The black dashed curve marks the boundary between the unbroken and broken regimes, defined by the condition  $\Re[-i\lambda_+] = 0$ . The red diamonds denote the EPs, while the blue, black, green, and orange markers highlight the specific parameter points whose time-domain dynamics are shown in panels (d)–(f). As  $\gamma_b$  increases, the range of negative asymmetry  $\delta_r$  accessible in the unbroken phase widens, whereas the area corresponding to the broken regime shrinks, consistent with the constraint  $\alpha < \Re[-i\Omega] - \gamma_b$ .

Figures 3(d)–(f) display the corresponding battery-charging dynamics for the same values of  $\gamma_b$  at the parameter points indicated in the phase diagrams. The purple region marks the boundary between the two regimes, corresponding to the purple star in Figs. 3(a)–(c). The behavior is fully consistent with the phase structure. Whenever the selected point lies in the broken regime, the battery energy grows exponentially in time, whereas in the unbroken regime, the energy saturates to the steady-state value given by  $\lim_{t \rightarrow \infty} E_B^{\text{un}}(t) = (\frac{\mathcal{E}_r}{\mathcal{K}})^2$ .

Figures 3(g)–(i) show the normalized rate of energy change in the battery,  $P_B(t)/\mathcal{E}_r^2$ , with  $P_B(t) = dE_B(t)/dt$ . This quantity indicates how quickly energy flows into or out of the battery. The difference between the two regimes is immediately visible. In the broken regime,  $P_B(t)$  increases exponentially, reflecting the rapid amplification driven by the unstable eigenmode. In contrast, in the unbroken regime the rate remains bounded and gradually decreases to zero as the system approaches its steady state.

In summary, exceptional points provide a powerful lens through which to understand and control the energy flow in the open quantum systems. In this work we have shown that exceptional-point behavior can be realized and harnessed in a fully passive, trace-preserving quantum platform, without requiring explicit gain, non-Hermitian Hamiltonians, or amplification mechanisms. By engineering a reservoir that mediates dissipative interference between the two quantum modes, we induce spectral coalescence and the resulting dynamical phase transition, enabling operation either in a stable regime with steady-state energy saturation or in a regime of sharply enhanced charging. The broken regime provides

a substantial boost in the rate of energy transfer, causing the stored energy to grow exponentially even under a bounded coherent drive. Although this large amplification is advantageous for rapid charging, its magnitude must be controlled in practice to prevent runaway dynamics or saturation of device components (see Supplementary Material II). This can be achieved through several strategies, such as dynamically tuning the system away from the exceptional point once a target energy is reached, introducing a soft upper-bound through weak nonlinearities or controlled dissipation, or incorporating real-time feedback that limits the effective coupling strength in the broken regime.

Our results establish a fundamentally new route to quantum batteries, where charging performance is enhanced not by strong nonlinearities or external gain, but through dissipatively generated exceptional points embedded directly within an open quantum device. Reservoir engineering renders the approach broadly compatible with numerous experimental platforms, including optomechanical, superconducting, and magnonic architectures, all of which offer long coherence times, high tunability, and strong hybrid interactions suitable for implementing exceptional-point-assisted energy storage.

The implications extend well beyond quantum batteries. Exceptional points mediated by engineered dissipation offer a versatile tool for shaping energy flow, coherence, and modal structure in quantum systems. This creates opportunities for quantum-limited amplification without gain media, noise-resilient transduction, enhanced sensing strategies, and topologically informed control of dissipative dynamics. Because the mechanism relies solely on passive, physical reservoirs, it avoids the fragility of traditional gain–loss implementations and is naturally robust against pump depletion, saturation, and uncontrolled instability. The ability to engineer and regulate dynamical phase transitions through reservoir design provides a new degree of control over energy exchange in quantum technologies, offering a blueprint for next-generation architectures in quantum information processing, sensing, communication, and energy science.

*Acknowledgements*— BA and PH acknowledge support from IRA Programme (project no. FENG.02.01-IP.05-0006/23) financed by the FENG program 2021–2027, Priority FENG.02, Measure FENG.02.01., with the support of the FNP. A.H.A.M. acknowledges support from National Science Centre, Poland Grant OPUS-21 (No. 2021/41/B/ST2/03207). PM acknowledges support by the Polish National Agency for Academic Exchange (NAWA), under Strategic Partnerships Programme, project number BNI/PST/2023/1/00013/U/00001. S.B. acknowledges funding by the Natural Sciences and Engineering Research Council of Canada (NSERC) through its Discovery Grant.

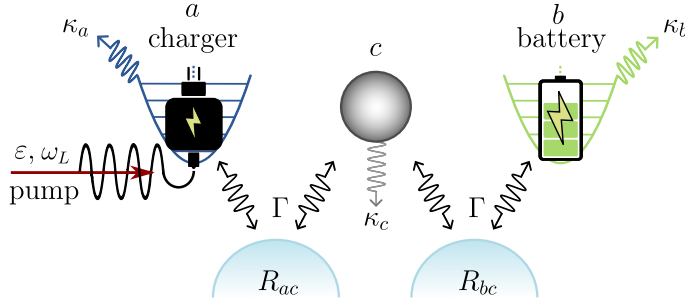


FIG. 4: Schematic representation of the charging process. The charger  $a$  is externally pumped by a laser field with amplitude  $\varepsilon$  and frequency  $\omega_L$ . The battery  $b$  charging is then mediated by a dissipative auxiliary mode  $c$ , individually connected to  $a$  and  $b$  through shared reservoirs  $R_{ac}$  and  $R_{bc}$  with coupling rate  $\Gamma$ . Each element has a local damping rate  $\kappa_{a/b/c}$ . The strongly overdamped auxiliary mode leads to an effective dissipative interaction between the charger and the battery.

#### Supplementary Materials for "Reservoir-Engineered Exceptional Points for Quantum Energy Storage"

## I. ANALYSIS OF SYSTEM ENERGY $E_B(t) = |b(t)|^2$

As schematically displayed in Fig. 4, our setting consists of three non-interacting harmonic oscillators, a charger  $a$ , a battery  $b$ , and an auxiliary system  $c$ . Each element is coupled to local environments at zero temperature, while  $a(b)$  and  $c$  are indirectly coupled through separate engineered shared-reservoirs. Additionally, a laser field with amplitude  $\varepsilon$  is shined onto  $a$  to feed energy into the system. Hence, an effective interaction between  $a$  and  $b$  can be realized, leading to battery charging (illustrated in Fig. 4). The total Hamiltonian of the system reads

$$\hat{H}_0 = \delta_a \hat{a}^\dagger \hat{a} + \delta_b \hat{b}^\dagger \hat{b} + \delta_c \hat{c}^\dagger \hat{c} + \mathcal{E} (\hat{a}^\dagger + \hat{a}) \quad (8)$$

where  $\delta_j \equiv \omega_j - \omega_L$  with  $j = a, b, c$  being the local detunings and  $\omega_L$  the frequency of the laser field. Its dynamics is then described by the following master equation [44, 63]

$$\begin{aligned} \frac{d\hat{\rho}}{dt} = & -i[\hat{H}_0, \hat{\rho}] + \kappa_a \mathcal{D}_a[\hat{\rho}] + \kappa_b \mathcal{D}_b[\hat{\rho}] + \kappa_c \mathcal{D}_c[\hat{\rho}] \\ & + \Gamma \mathcal{D}_{z_a}[\hat{\rho}] + \Gamma \mathcal{D}_{z_b}[\hat{\rho}], \end{aligned} \quad (9)$$

where  $\mathcal{D}_o[\cdot] = \hat{o} \cdot \hat{o}^\dagger - \frac{1}{2}\{\hat{o}^\dagger \hat{o}, \cdot\}$  represents the dissipative super-operator resulting from the coupling to the reservoirs. Here,  $\kappa_j$  corresponds to the dissipation rate caused by the local reservoirs  $j = a, b, c$  and  $\Gamma$  the dissipation rate at which a photon is absorbed and emitted by the common reservoir due to the coupling  $\hat{z}_m = p_m \hat{m} + p_c^m \hat{c}$  with  $m = a, b$ . Here,  $\hat{z}_m$  describes the coupling of the charger and battery to the shared reservoir, respectively [59].

Exploiting the master equation (9), we obtain the following set of equations of motion for the first moments,  $o := \text{Tr}\{\hat{o}\hat{\rho}\}$  with  $x = a, b$ , as

$$\frac{da}{dt} = -i[\delta - i(k_a + \Gamma_a)]a - \mu_{ca}\Gamma c + \varepsilon, \quad (10)$$

$$\frac{db}{dt} = -i[-\delta - i(k_b + \Gamma_b)]b - \mu_{cb}\Gamma c, \quad (11)$$

$$\frac{dc}{dt} = -(k_c + \Gamma_c^a + \Gamma_c^b)c - \Gamma(\mu_{ca}^*a + \mu_{cb}^*b), \quad (12)$$

where  $\Gamma_i = \Gamma|p_i|^2$ ,  $\Gamma_c^i = \Gamma|p_c^i|^2$  and  $\mu_{ci} = p_c^i p_i^*$  with  $i = a, b$ . We assumed  $\delta_a = -\delta_b = \delta$ , and  $\delta_c = 0$ . For simplicity, we consider  $\mu_{ca(b)} = \mu$  in the following. Assuming  $k_c + \Gamma_c^a + \Gamma_c^b \gg k_{a(b)} + \Gamma_{a(b)} + \delta_{a(b)}$  allows us to perform the adiabatic elimination of mode  $c$  as

$$\frac{dc}{dt} = 0 \Rightarrow c = -\frac{\Gamma}{k_c + \Gamma_c^a + \Gamma_c^b}(\mu^*a + \mu^*b), \quad (13)$$

which means that mode  $c$  quickly thermalizes compared to the time-scale over which the charger and the battery states change significantly. Substituting this equation into Eqs. (10) and (11) we arrive at a simpler set of coupled

differential equations

$$\frac{da}{dt} = -i\Gamma_{\text{eff}}(\delta_r - i\gamma_a)a + |\mu|^2\Gamma_{\text{eff}}b + \varepsilon, \quad (14)$$

$$\frac{db}{dt} = -i\Gamma_{\text{eff}}(-\delta_r - i\gamma_b)b + |\mu|^2\Gamma_{\text{eff}}a, \quad (15)$$

where  $\gamma_j = \Gamma_{\text{eff}}^{-1}(\kappa_j + \Gamma_j - |\mu|^2\Gamma_{\text{eff}})$  with  $\delta_r = \delta/\Gamma_{\text{eff}}$  and

$$\Gamma_{\text{eff}} = \frac{\Gamma^2}{k_c + \Gamma_c^a + \Gamma_c^b}. \quad (16)$$

In this section, we analyze the energy of system  $B$ ,  $E_B(t) = |b(t)|^2$ , without assuming symmetric damping and coupling rates (i.e.,  $\kappa_a \neq \kappa_b$  and  $\Gamma_a \neq \Gamma_b$ ). The dynamical equation for the system is, therefore,

$$\frac{1}{\Gamma_{\text{eff}}} \frac{d}{dt} \begin{pmatrix} a \\ b \end{pmatrix} = -i\mathbb{H}_r \begin{pmatrix} a \\ b \end{pmatrix} + \begin{pmatrix} \mathcal{E}_r \\ 0 \end{pmatrix}, \quad (17)$$

where  $\mathcal{E}_r = \mathcal{E}/\Gamma_{\text{eff}}$  and the normalized matrix  $\mathbb{H}_r$  is

$$\mathbb{H}_r = \begin{pmatrix} \delta_r - i\gamma_a & i \\ i & -\delta_r - i\gamma_b \end{pmatrix}. \quad (18)$$

Rescaling the time  $t$  as  $t \rightarrow \Gamma_{\text{eff}}t$  allows us to be working with the normalized matrix  $\mathbb{H}_r$  in the following. Consider  $A(t) = [a(t), b(t)]^T$  and  $C = [\mathcal{E}_r, 0]^T$ , the general solution for Eq. (17) is given by:

$$A(t) = e^{-i\mathbb{H}_r t} A(t_0) + \int_0^t e^{-i\mathbb{H}_r(t-\tau)} C d\tau, \quad (19)$$

where the first term on the right is referred to as the homogeneous solution and the second term as the inhomogeneous term. With the ground state as the initial condition, i.e.,  $a(t=0) = 0$ ,  $b(t=0) = 0$ , the first term plays no role in the evolution. The eigenvalues of  $\mathbb{H}_r$ , denoted by  $\lambda_{\pm}$ , are found from the characteristic equation  $\det(\mathbb{H}_r - \lambda I) = 0$ , which yields a quadratic equation:

$$\lambda^2 + 2i(\alpha + \gamma_b)\lambda - 2\alpha(\gamma_b - i\delta_r) - (\gamma_b^2 + \delta_r^2) + 1 = 0, \quad (20)$$

where  $\alpha = (\gamma_a - \gamma_b)/2$  is the coefficient of asymmetry. The solutions for the eigenvalues are given by

$$\lambda_{\pm} = -i(\alpha + \gamma_b) \pm \Omega, \quad \Omega = i\sqrt{1 + (\alpha + i\delta_r)^2}. \quad (21)$$

It is important to highlight the nature of the solutions for  $a(t)$  and  $b(t)$  strongly depend on the real and imaginary components of  $\lambda_{\pm}$ . Fig. 5 shows how these quantities behave in terms of  $\alpha$  and  $\delta_r$ . In particular, note that  $\gamma_b \in \mathbb{R}^+$  only influences the imaginary component of the eigenvalues. More importantly, it implies that  $\Im[\lambda_-] \leq 0$  for all values of  $\alpha$ ,  $\delta_r$  and  $\gamma_b$ . The matrix exponential  $e^{-i\mathbb{H}_r \xi}$ , with  $\xi$  being a scalar, is given by:

$$e^{-i\mathbb{H}_r \xi} = \frac{e^{-i\lambda_+ \xi}(\mathbb{H}_r - (-i)\lambda_- I) - e^{-i\lambda_- \xi}(\mathbb{H}_r - (-i)\lambda_+ I)}{-i(\lambda_+ - \lambda_-)}. \quad (22)$$

This method for computing  $e^{-i\mathbb{H}_r \xi}$  whenever  $\mathbb{H}_r$  has distinct eigenvalues is a standard result in linear algebra and matrix theory, often derived from Sylvester's formula or by considering the Cayley-Hamilton theorem, which states that a matrix satisfies its own characteristic polynomial. Substituting the expressions for  $\mathbb{H}_r$ ,  $\lambda_{\pm}$ , and using the equality  $\lambda_+ - \lambda_- = 2\Omega$ , the elements of  $e^{-i\mathbb{H}_r \tau} = \begin{pmatrix} m_{11}(\tau) & m_{12}(\tau) \\ m_{21}(\tau) & m_{22}(\tau) \end{pmatrix}$  are obtained as

$$\begin{aligned} m_{11}(\tau) &= \frac{1}{2\Omega} \left[ \left( \frac{-2i\delta + \gamma_b - \gamma_a}{2} \right) (e^{-i\lambda_+ \tau} - e^{-i\lambda_- \tau}) + \left( \frac{2\Omega}{2} \right) (e^{-i\lambda_+ \tau} + e^{-i\lambda_- \tau}) \right], \\ m_{12}(\tau) &= \frac{1}{2\Omega} (e^{-i\lambda_+ \tau} - e^{-i\lambda_- \tau}), \\ m_{21}(\tau) &= \frac{1}{2\Omega} (e^{-i\lambda_+ \tau} - e^{-i\lambda_- \tau}), \\ m_{22}(\tau) &= \frac{1}{2\Omega} \left[ \left( \frac{2i\delta + \gamma_a - \gamma_b}{2} \right) (e^{-i\lambda_+ \tau} - e^{-i\lambda_- \tau}) + \left( \frac{2\Omega}{2} \right) (e^{-i\lambda_+ \tau} + e^{-i\lambda_- \tau}) \right]. \end{aligned} \quad (23)$$

We are particularly interested in  $b(t) = \mathcal{E} \int_0^t m_{21}(\tau) d\tau$ .

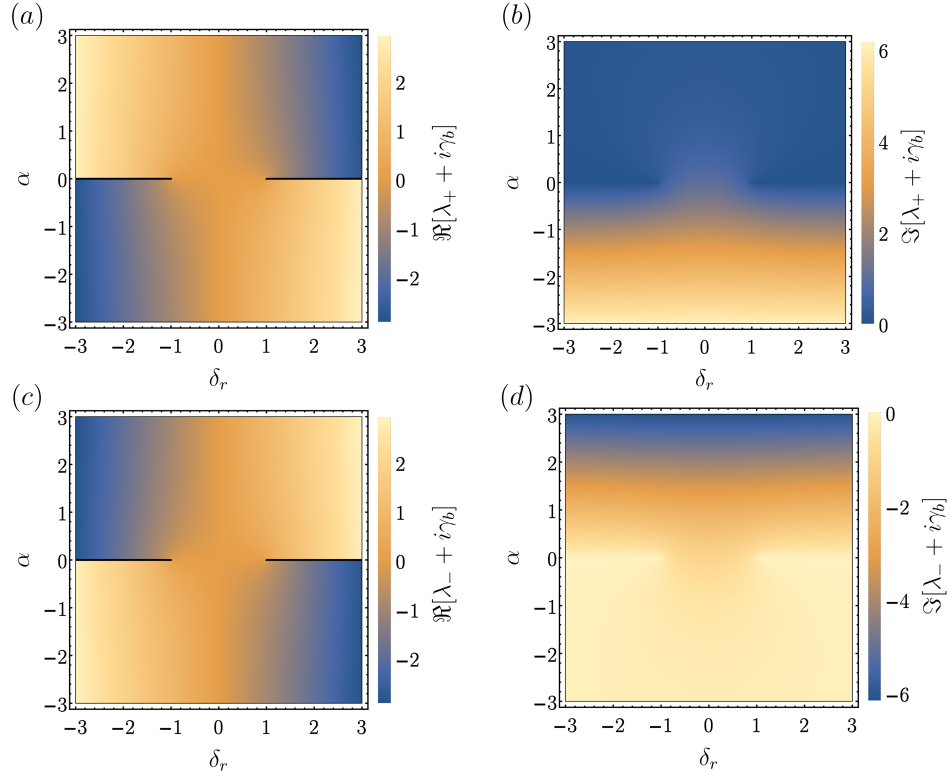


FIG. 5: (a)-(c) Real and (b)-(d) imaginary parts of the eigenvalues  $\lambda_{\pm}$  displaced by  $i\gamma_b$  as a function of  $\delta_r = \delta/\Gamma_{\text{eff}}$  and the coefficient of asymmetry  $\alpha := (\gamma_a - \gamma_b)/2$ . The black line in (a) and (c) highlights the discontinuity in the real components.

### A. Case 1: Exceptional Point (EP) Regime ( $\Omega = 0$ )

An EP (where eigenvalues coalesce, i.e.,  $\Omega = 0$ ) in the non-symmetric case is generally quite restrictive. It requires both the real and imaginary parts of  $\Omega$  to be zero:

$$\begin{aligned} (\gamma_a - \gamma_b)^2 - 4(\delta_r^2 - 1) &= 0, \\ -4\delta_r(\gamma_b - \gamma_a) &= 0. \end{aligned}$$

The second condition implies either  $\delta_r = 0$  or  $\gamma_a = \gamma_b$ . If  $\delta_r = 0$ , the first condition becomes  $(\gamma_a - \gamma_b)^2 + 4 = 0$ . Since  $\gamma_a, \gamma_b$  and  $\Gamma_{\text{eff}}$  are real this relation cannot be zero. Therefore, a true EP in the non-symmetric case necessitates  $\gamma_a = \gamma_b$ . This implies  $k_a + \Gamma_a = k_b + \Gamma_b$ . If this holds, the first condition simplifies to  $4(\delta_r^2 - 1) = 0$ , meaning  $\delta_r = \pm 1$ . Thus, an EP occurs only if the system's effective diagonal terms are balanced ( $k_a + \Gamma_a = k_b + \Gamma_b$ ) and the detuning matches the effective coupling ( $\delta_r = \pm 1$ ). When  $\Omega = 0$ , the eigenvalues coalesce to  $\lambda_0 = \frac{\gamma_a + \gamma_b}{2}$ . Since  $\gamma_a = \gamma_b$  is required for an EP,  $\lambda_0 = -i\gamma_a$ , which is a real number. For a  $2 \times 2$  matrix, if there is a repeated eigenvalue  $\lambda_0$  and only one linearly independent eigenvector,  $\mathbb{H}_r$  can be written as  $PJP^{-1}$ , where

$$J = \begin{pmatrix} \lambda_0 & 1 \\ 0 & \lambda_0 \end{pmatrix} \quad (24)$$

is called a Jordan block matrix. The exponential of a Jordan block  $J$  is:

$$e^{J\tau} = \begin{pmatrix} e^{\lambda_0\tau} & \tau e^{\lambda_0\tau} \\ 0 & e^{\lambda_0\tau} \end{pmatrix} = e^{\lambda_0\tau} \begin{pmatrix} 1 & \tau \\ 0 & 1 \end{pmatrix}. \quad (25)$$

This can be rewritten as:

$$\begin{aligned} e^{J\tau} &= e^{\lambda_0\tau} \left( I + \begin{pmatrix} 0 & \tau \\ 0 & 0 \end{pmatrix} \right) \\ &= e^{\lambda_0\tau} (I + (J - \lambda_0 I)\tau). \end{aligned} \quad (26)$$

Since  $e^{-i\mathbb{H}_r\tau} = Pe^{-iJ\tau}P^{-1}$ , we can substitute the expression for  $e^{-iJ\tau}$ :

$$\begin{aligned} e^{-i\mathbb{H}_r\tau} &= P \left( e^{-i\lambda_0\tau} (I - i(J - \lambda_0 I)\tau) \right) P^{-1} \\ &= e^{-i\lambda_0\tau} (I - iP(J - \lambda_0 I)P^{-1}\tau). \end{aligned}$$

Using the relation  $PJP^{-1} = \mathbb{H}_r$ , we get  $P(J - \lambda_0 I)P^{-1} = \mathbb{H}_r - \lambda_0 I$ . Thus, the matrix exponential becomes

$$e^{-i\mathbb{H}_r\tau} = e^{-i\lambda_0\tau} (I - i(\mathbb{H}_r - \lambda_0 I)\tau). \quad (27)$$

Substituting  $\mathbb{H}_r - \lambda_0 I = \begin{pmatrix} \delta_r & i \\ i & -\delta_r \end{pmatrix}$  (since  $\gamma_a = \gamma_b$ ), the elements of  $e^{-i\mathbb{H}_r\tau}$  reads

$$\begin{aligned} m_{11}(\tau) &= e^{-i\lambda_0\tau} (1 - i\delta_r\tau), \\ m_{12}(\tau) &= e^{-i\lambda_0\tau} \tau, \\ m_{21}(\tau) &= e^{-i\lambda_0\tau} \tau, \\ m_{22}(\tau) &= e^{-i\lambda_0\tau} (1 + i\delta_r\tau). \end{aligned} \quad (28)$$

The solutions for  $a(t)$  and  $b(t)$  are obtained by integrating the corresponding elements of the matrix exponential from 0 to  $t$ . We use the standard integral forms:  $\int_0^t e^{ax} dx = \frac{e^{at}-1}{a}$  and  $\int_0^t x e^{ax} dx = \frac{x e^{ax}}{a} - \frac{e^{ax}-1}{a^2}$  (for  $a \neq 0$ ). Then the solution for  $b(t)$  in this specific EP scenario is

$$b(t) = \mathcal{E}_r \left[ \frac{ie^{-i\lambda_0 t}}{\lambda_0} \left( t - \frac{i}{\lambda_0} \right) - \frac{1}{\lambda_0^2} \right]. \quad (29)$$

The energy of the battery  $B$  is then computed as  $E_B(t) = |b(t)|^2$ .

### B. Case 2: Distinct Eigenvalues Regime ( $\Omega \neq 0$ )

In the general non-symmetric case,  $\Omega$  is typically a complex number, leading to distinct complex eigenvalues  $\lambda_{\pm}$  that are not necessarily complex conjugates. This means the standard classification into "Unbroken" (oscillatory, identical imaginary parts of  $\mathbb{H}$  eigenvalues) and "Broken" (exponential, distinct imaginary parts of  $\mathbb{H}$  eigenvalues) phases becomes less straightforward and often requires deeper analysis of the full eigenvalue spectrum of  $\mathbb{H}$ . Using Eqs. (22) and (23) the general analytical solution for  $b(t)$  when  $\Omega \neq 0$  reads

$$b(t) = \frac{\mathcal{E}_r}{\lambda_+ \lambda_- (\lambda_+ - \lambda_-)} [\lambda_+ e^{-i\lambda_- t} - \lambda_- e^{-i\lambda_+ t} - (\lambda_+ - \lambda_-)], \quad (30)$$

where  $\lambda_{\pm} = -i(\gamma_a + \gamma_b) \pm i\Omega$ . The energy  $E_B(t)$  is given by  $E_B(t) = |b(t)|^2$ . In this case,  $b(t)$  will generally be a complex-valued function of time.

## II. OPERATIONAL LIMITS AND SAFETY PROTOCOLS IN THE BROKEN PHASE

While the broken phase facilitates exponential energy storage, practical implementation requires terminating the charging process before the stored energy exceeds the device's physical breakdown threshold, denoted as  $E_{\max}$ . Here, we derive the critical operation time,  $t_{\text{crit}}$ , based on the exact dynamics of the broken regime. Starting from the energy expression for the broken phase (with  $\alpha = 0$ ):

$$E_B^{\text{br}}(t) = \frac{\mathcal{E}_r^2}{\mathcal{K}^2} \left( 1 - \frac{e^{-\gamma t}}{|\Omega|} [\gamma \sinh(|\Omega|t) + |\Omega| \cosh(|\Omega|t)] \right)^2, \quad (31)$$

where  $\mathcal{K} = \delta_r^2 + \gamma^2 - 1$  and  $|\Omega| = \sqrt{1 - \delta_r^2}$ . In the asymptotic limit where charging is substantial ( $t \gg |\Omega|^{-1}$ ), the hyperbolic terms are dominated by the growing exponential,  $\sinh(x) \approx \cosh(x) \approx e^x/2$ . Consequently, the energy evolution simplifies to:

$$E_B^{\text{br}}(t) \approx \frac{\mathcal{E}_r^2}{\mathcal{K}^2} \left( \frac{\gamma + |\Omega|}{2|\Omega|} \right)^2 e^{2(|\Omega| - \gamma)t}. \quad (32)$$

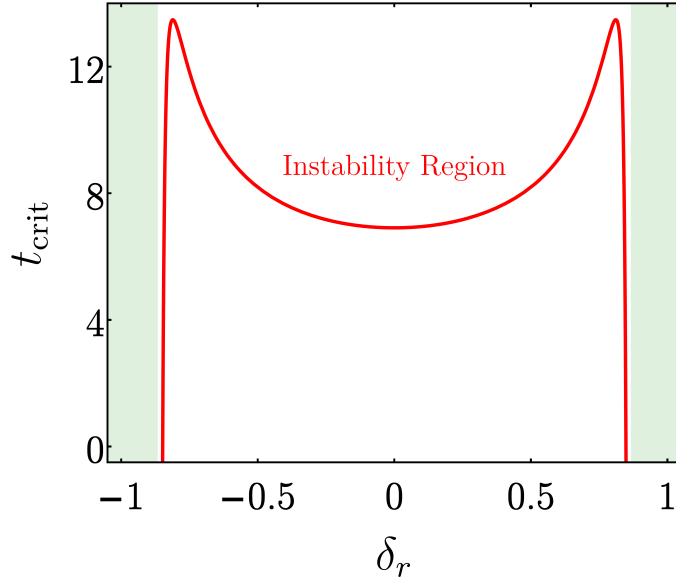


FIG. 6: **Operational limits in the broken phase.** The critical time  $t_{\text{crit}}$  required for the battery energy to reach the safety threshold  $E_{\text{max}}$  as a function of the normalized detuning  $\delta_r$ , derived from Eq. (31). Green shaded regions indicate the stable (unbroken) phase. The sharp drop near the phase boundaries ( $\delta_r \approx \pm 0.866$ ) results from the divergence of the steady-state amplitude scaling factor  $\mathcal{K}^{-2}$ , causing the baseline energy to exceed  $E_{\text{max}}$  instantaneously. Parameters:  $\alpha = 0$ ,  $\gamma_b = 0.5$ , and  $E_{\text{max}} = 10^3 \mathcal{E}_r^2$ .

Defining  $t_{\text{crit}}$  as the time at which  $E_B^{\text{br}}(t) = E_{\text{max}}$ , we solve for  $t$  to obtain the operational limit:

$$t_{\text{crit}} \approx \frac{1}{2(|\Omega| - \gamma)} \ln \left( \frac{E_{\text{max}}}{E_{\text{scale}}} \right), \quad (33)$$

where the energy scaling factor is  $E_{\text{scale}} = \frac{\mathcal{E}_r^2}{4\mathcal{K}^2} \left( \frac{\gamma + |\Omega|}{|\Omega|} \right)^2$ .

This analytical result highlights two key physical constraints. First, the denominator  $2(|\Omega| - \gamma)$  represents the system's effective net gain; as dissipative interference strengthens (larger  $|\Omega|$ ), the charging rate increases, inversely shortening the safe operating window. Second, the logarithmic dependence on  $E_{\text{max}}/E_{\text{scale}}$  implies that increasing the hardware's breakdown voltage yields only diminishing returns on the charging duration, emphasizing the need for precise timing over material hardening.

The dependence of  $t_{\text{crit}}$  on detuning, shown in Fig. 6, reveals distinct operational regimes. While the central resonance ( $\delta_r = 0$ ) offers the fastest charging, it imposes the strictest timing constraints on control circuitry. Conversely, the intermediate detunings (the “shoulders” of the plot) provide a “safe harbor.” In these regions, the system retains exponential growth properties but offers a critical time window nearly double that of the resonance point, significantly reducing the risk of accidental damage. Experimentally,  $t_{\text{crit}}$  defines the trigger point for a safety protocol: applying a detuning pulse at  $t < t_{\text{crit}}$  shifts the system back into the unbroken phase (where  $\Omega$  is real), instantly halting exponential growth and locking the stored energy in a stable state.

Future analysis will address the dynamics of pulse switching, which is expected to influence the critical time, effective power, and charging efficiency. In particular, rapid switching regimes may necessitate theoretical treatments beyond the standard Markovian model.

---

[1] W. D. Heiss, The physics of exceptional points, *Journal of Physics A: Mathematical and Theoretical* **45**, 444016 (2012).

[2] Y. Ashida, Z. Gong, and M. Ueda, Non-hermitian physics, *Advances in Physics* **69**, 249 (2020).

[3] R. El-Ganainy, K. G. Makris, M. Khajavikhan, Z. H. Musslimani, S. Rotter, and D. N. Christodoulides, Non-hermitian physics and PT symmetry, *Nature Physics* **14**, 11 (2018).

[4] S. K. Özdemir, S. Rotter, F. Nori, and L. Yang, Parity-time symmetry and exceptional points in photonics, *Nature Materials* **18**, 783 (2019).

[5] S. Barzanjeh, A. Xuereb, A. Alù, S. A. Mann, N. Nefedkin, V. Peano, and P. Rabl, Nonreciprocity in quantum technology (2025), [arXiv:2508.03945](https://arxiv.org/abs/2508.03945).

[6] W. Chen, S. K. Ozdemir, G. Zhao, J. Wiersig, and L. Yang, Exceptional points enhance sensing in an optical microcavity, *Nature* **548**, 192 (2017).

[7] M.-A. Miri and A. Alù, Exceptional points in optics and photonics, *Science* **363**, eaar7709 (2019).

[8] J.-H. Park, A. Ndao, W. Cai, L. Hsu, A. Kodigala, T. Lepetit, Y.-H. Lo, and B. Kanté, Symmetry-breaking-induced plasmonic exceptional points and nanoscale sensing, *Nature Physics* **16**, 462 (2020).

[9] W. Tang, X. Jiang, K. Ding, Y.-X. Xiao, Z.-Q. Zhang, C. T. Chan, and G. Ma, Exceptional nexus with a hybrid topological invariant, *Science* **370**, 1077 (2020).

[10] H. Zhou, C. Peng, Y. Yoon, C. W. Hsu, K. A. Nelson, L. Fu, J. D. Joannopoulos, M. Soljačić, and B. Zhen, Observation of bulk fermi arc and polarization half charge from paired exceptional points, *Science* **359**, 1009 (2018).

[11] C. E. Rüter, K. G. Makris, R. El-Ganainy, D. N. Christodoulides, M. Segev, and D. Kip, Observation of parity-time symmetry in optics, *Nature Physics* **6**, 192 (2010).

[12] L. Feng, Y.-L. Xu, W. S. Fegadolli, M.-H. Lu, J. E. B. Oliveira, V. R. Almeida, Y.-F. Chen, and A. Scherer, Experimental demonstration of a unidirectional reflectionless parity-time metamaterial at optical frequencies, *Nature Materials* **12**, 108 (2013).

[13] L. Feng, Z. J. Wong, R.-M. Ma, Y. W. Wang, and X. Zhang, Single-mode laser by parity-time symmetry breaking, *Science* **346**, 972 (2014).

[14] H. Hodaei, M.-A. Miri, M. Heinrich, D. N. Christodoulides, and M. Khajavikhan, Parity-time-symmetric microring lasers, *Science* **346**, 975 (2014).

[15] W. R. Sweeney, C. W. Hsu, S. Rotter, and A. D. Stone, Perfectly absorbing exceptional points and chiral absorbers, *Phys. Rev. Lett.* **122**, 093901 (2019).

[16] C. Wang, W. R. Sweeney, A. D. Stone, and L. Yang, Coherent perfect absorption at an exceptional point, *Science* **373**, 1261 (2021).

[17] H. Xu, D. Mason, L. Jiang, and J. Harris, Topological energy transfer in an optomechanical system with exceptional points, *Nature* **537**, 80 (2016).

[18] M. Naghiloo, M. Abbasi, Y. N. Joglekar, and K. W. Murch, Quantum state tomography across the exceptional point in a single dissipative qubit, *Nature Physics* **15**, 1232 (2019).

[19] X. Yu and C. Zhang, Quantum parameter estimation of non-hermitian systems with optimal measurements, *Phys. Rev. A* **108**, 022215 (2023).

[20] R. Alicki and M. Fannes, Entanglement boost for extractable work from ensembles of quantum batteries, *Phys. Rev. E* **87**, 042123 (2013).

[21] A. Camposeo, T. Virgili, F. Lombardi, G. Cerullo, D. Pisignano, and M. Polini, Quantum batteries: A materials science perspective, *Advanced Materials* **37**, 2415073 (2025).

[22] F. Campaioli, S. Gherardini, J. Q. Quach, M. Polini, and G. M. Andolina, Colloquium: Quantum batteries, *Rev. Mod. Phys.* **96**, 031001 (2024).

[23] S. Gherardini, F. Campaioli, F. Caruso, and F. C. Binder, Stabilizing open quantum batteries by sequential measurements, *Phys. Rev. Res.* **2**, 013095 (2020).

[24] A. H. Malavazi, R. Sagar, B. Ahmadi, and P. R. Dieguez, Two-time weak-measurement protocol for ergotropy protection in open quantum batteries, *PRX Energy* **4**, 023011 (2025).

[25] B. Ahmadi, A. B. Ravichandran, P. Mazurek, S. Barzanjeh, and P. Horodecki, Harnessing environmental noise for quantum energy storage, [arXiv:2510.06384](https://arxiv.org/abs/2510.06384) (2025).

[26] J. Q. Quach, K. E. McGhee, L. Ganzer, D. M. Rouse, B. W. Lovett, E. M. Gauger, J. Keeling, G. Cerullo, D. G. Lidzey, and T. Virgili, Superabsorption in an organic microcavity: Toward a quantum battery, *Science Advances* **8**, 3160 (2022).

[27] J. Q. Quach and W. J. Munro, Using dark states to charge and stabilize open quantum batteries, *Phys. Rev. Appl.* **14**, 024092 (2020).

[28] X. Yang, Y.-H. Yang, M. Alimuddin, R. Salvia, S.-M. Fei, L.-M. Zhao, S. Nimmrichter, and M.-X. Luo, Battery capacity of energy-storing quantum systems, *Phys. Rev. Lett.* **131**, 030402 (2023).

[29] D. Ferraro, M. Campisi, G. M. Andolina, V. Pellegrini, and M. Polini, High-power collective charging of a solid-state quantum battery, *Phys. Rev. Lett.* **120**, 117702 (2018).

[30] R. R. Rodríguez, B. Ahmadi, P. Mazurek, S. Barzanjeh, R. Alicki, and P. Horodecki, Catalysis in charging quantum batteries, *Phys. Rev. A* **107**, 042419 (2023).

[31] D. Rinaldi, R. Filip, D. Gerace, and G. Guarneri, Reliable quantum advantage in quantum battery charging, *Phys. Rev. A* **112**, 012205 (2025).

[32] R. Salvia, M. Perarnau-Llobet, G. Haack, N. Brunner, and S. Nimmrichter, Quantum advantage in charging cavity and spin batteries by repeated interactions, *Phys. Rev. Res.* **5**, 013155 (2023).

[33] R. R. Rodríguez, B. Ahmadi, G. Suárez, P. Mazurek, S. Barzanjeh, and P. Horodecki, Optimal quantum control of charging quantum batteries, *New Journal of Physics* **26**, 043004 (2024).

[34] F.-M. Yang and F.-Q. Dou, Wireless energy transfer in a non-hermitian quantum battery, *Phys. Rev. A* **112**, 042205 (2025).

[35] T. K. Konar, L. G. C. Lakkaraju, and A. Sen (De), Quantum battery with non-hermitian charging, *Phys. Rev. A* **109**, 042207 (2024).

[36] Z.-G. Lu, G. Tian, X.-Y. Lü, and C. Shang, Topological quantum batteries, *Phys. Rev. Lett.* **134**, 180401 (2025).

[37] X.-L. Zhang, X.-K. Song, and D. Wang, Quantum battery in the heisenberg spin chain models with dzyaloshinskii-moriya interaction, *Advanced Quantum Technologies* **7**, 2400114 (2024).

[38] F. Barra, Dissipative charging of a quantum battery, *Phys. Rev. Lett.* **122**, 210601 (2019).

[39] F. T. Tabesh, F. H. Kamin, and S. Salimi, Environment-mediated charging process of quantum batteries, *Phys. Rev. A* **102**, 052223 (2020).

[40] S. Ghosh, T. Chanda, S. Mal, and A. Sen(De), Fast charging of a quantum battery assisted by noise, *Phys. Rev. A* **104**, 032207 (2021).

[41] F. Mayo and A. J. Roncaglia, Collective effects and quantum coherence in dissipative charging of quantum batteries, *Phys. Rev. A* **105**, 062203 (2022).

[42] K. Xu, H.-J. Zhu, G.-F. Zhang, and W.-M. Liu, Enhancing the performance of an open quantum battery via environment engineering, *Phys. Rev. E* **104**, 064143 (2021).

[43] B. Ahmadi, P. Mazurek, P. Horodecki, and S. Barzanjeh, Nonreciprocal quantum batteries, *Phys. Rev. Lett.* **132**,

210402 (2024).

[44] B. Ahmadi, P. Mazurek, S. Barzanjeh, and P. Horodecki, Superoptimal charging of quantum batteries via reservoir engineering: Arbitrary energy transfer unlocked, *Phys. Rev. Appl.* **23**, 024010 (2025).

[45] R. Shastri, C. Jiang, G.-H. Xu, B. Prasanna Venkatesh, and G. Watanabe, Dephasing enabled fast charging of quantum batteries, *npj Quantum Information* **11**, 9 (2025).

[46] M.-L. Hu, T. Gao, and H. Fan, Efficient wireless charging of a quantum battery, *Phys. Rev. A* **111**, 042216 (2025).

[47] A. H. Malavazi, B. Ahmadi, P. Horodecki, and P. R. Dieguez, Charge-preserving operations in quantum batteries, *arXiv:2510.25549* (2025).

[48] S. Zakavati, S. Salimi, and B. Arash, Optimizing the charging of open quantum batteries using long short-term memory-driven reinforcement learning, *arXiv:2504.19840* (2025).

[49] J. F. Poyatos, J. I. Cirac, and P. Zoller, Quantum reservoir engineering with laser cooled trapped ions, *Physical Review Letters* **77**, 4728 (1996).

[50] M. Müller, K. Hammerer, Y. Zhou, C. F. Roos, and P. Zoller, Quantum state preparation via engineered dissipation in open quantum systems, *Science* **351**, 273 (2016).

[51] A. Metelmann and A. A. Clerk, Nonreciprocal photon transmission and amplification via reservoir engineering, *Physical Review X* **5**, 021025 (2015).

[52] A. Metelmann and A. A. Clerk, Using interference to engineer nonclassical states of light and mechanics, *Nature Physics* **12**, 1093 (2016).

[53] L. D. Toth, N. R. Bernier, A. Nunnenkamp, A. K. Fedorov, and T. J. Kippenberg, A dissipative quantum reservoir for microwave light using a mechanical oscillator, *Nat Phys* **13**, 787 (2017).

[54] S. Barzanjeh, M. Wulf, M. Peruzzo, M. Kalaei, P. B. Dieterle, O. Painter, and J. M. Fink, Mechanical on-chip microwave circulator, *Nature Communications* **8**, 953 (2017).

[55] J. Kerckhoff, K. Lalumière, B. J. Chapman, A. Blais, and K. W. Lehnert, On-chip superconducting microwave circulator from synthetic rotation, *Phys. Rev. Appl.* **4**, 034002 (2015).

[56] B. J. Chapman, E. I. Rosenthal, J. Kerckhoff, B. A. Moores, L. R. Vale, J. A. B. Mates, G. C. Hilton, K. Lalumière, A. Blais, and K. W. Lehnert, Widely tunable on-chip microwave circulator for superconducting quantum circuits, *Phys. Rev. X* **7**, 041043 (2017).

[57] Y.-P. Wang, J. W. Rao, Y. Yang, P.-C. Xu, Y. S. Gui, B. M. Yao, J. Q. You, and C.-M. Hu, Nonreciprocity and unidirectional invisibility in cavity magnonics, *Phys. Rev. Lett.* **123**, 127202 (2019).

[58] M. Kim, A. Tabesh, T. Zegray, S. Barzanjeh, and C.-M. Hu, Nonreciprocity in cavity magnonics at millikelvin temperature, *Journal of Applied Physics* **135** (2024).

[59] A. Metelmann and A. A. Clerk, Nonreciprocal photon transmission and amplification via reservoir engineering, *Phys. Rev. X* **5**, 021025 (2015).

[60] Y.-X. Wang, C. Wang, and A. A. Clerk, Quantum nonreciprocal interactions via dissipative gauge symmetry, *PRX Quantum* **4**, 010306 (2023).

[61] M. Aspelmeyer, T. J. Kippenberg, and F. Marquardt, Cavity optomechanics, *Rev. Mod. Phys.* **86**, 1391 (2014).

[62] E. X. DeJesus and C. Kaufman, Routh-hurwitz criterion in the examination of eigenvalues of a system of nonlinear ordinary differential equations, *Phys. Rev. A* **35**, 5288 (1987).

[63] H.-P. Breuer, F. Petruccione, *et al.*, *The theory of open quantum systems* (Oxford University, Oxford, 2007).